Available online at www.sciencedirect.com

ScienceDirect

Procedia Computer Science 1 (2012) 1931–1939

Procedia Computer Science

www.elsevier.com/locate/procedia

International Conference on Computational Science, ICCS 2010

A second-order compatible staggered Lagrangian hydrodynamics scheme using a cell-centered multidimensional approximate Riemann solver

Raphaël Loubère[1,*]

Université de Toulouse, Institut de Mathématiques de Toulouse et CNRS, France

Pierre-Henri Maire[*]

UMR CELIA, CNRS, Université Bordeaux 1, CEA, France.

Pavel Váchal[1,*]

Faculty of Nuclear Sciences and Physical Engineering, Czech Technical University in Prague, Czech Republic.

Abstract

We develop a general framework to derive and analyze staggered numerical schemes devoted to solve hydrodynamics equations in 2D. In this framework a cell-centered multi-dimensional approximate Riemann solver is used to build a form of artificial viscosity that leads to a conservative, compatible and thermodynamically consistent scheme. A second order extension in space and time for this scheme is proposed in this work and we prove on numerical examples the validity of this approach.

Keywords: Lagrangian hydrodynamics, artificial viscosity, Riemann solver, second order

2000 MSC: 35L75, 76N15, 76N99, 76L05, 65M06

1. Introduction

In this work we present new 2D compatible staggered Lagrangian hydrodynamics schemes. Their artificial viscosity is based on a cell-centered multidimensional approximate Riemann solver. This new formulation allows to link the newly developed cell-centered Lagrangian schemes [8] and the compatible staggered Lagrangian formulation

[*]Corresponding author: R. Loubère

Email addresses: raphael.loubere@math.univ-toulouse.fr (Raphaël Loubère), maire@celia.u-bordeaux1.fr (Pierre-Henri Maire), vachal@galileo.fjfi.cvut.cz (Pavel Váchal)

URL: http://loubere.free.fr (Raphaël Loubère), http://www.celia.u-bordeaux1.fr/~maire/ (Pierre-Henri Maire), http://kfe.fjfi.cvut.cz/~vachal/ (Pavel Váchal)

[1]This author has been supported by the Czech Ministry of Education grants MSM 6840770022, MSM 6840770010 and LC528

1877-0509
doi:10.1016/j.procs.2010.04.216

[6, 2]. Extensions to second order in space and time are the main contribution of this paper. Second order in space is obtained through the use of a piecewise linear reconstruction of the velocity field inside the force computation. Second order in time is gained thanks to a predictor-corrector scheme. The paper is organized as follows; first the compatible Lagrangian formalism is presented (equations, notation and Riemann solver) then the second order extension is introduced, finaly numerical examples are presented to assess the validity of this approach.

2. Compatible Lagrangian hydrodynamics

2.1. Governing equations.

In classical staggered Lagrangian framework [6, 2] one solves hydrodynamics equations written as

$$\rho \frac{d}{dt}\left(\frac{1}{\rho}\right) - \nabla \cdot \boldsymbol{U} = 0, \qquad \rho \frac{d}{dt}\boldsymbol{U} + \boldsymbol{\nabla} P = \boldsymbol{0}, \qquad \rho \frac{d}{dt}\varepsilon + P\nabla \cdot \boldsymbol{U} = 0, \tag{1}$$

where ρ is the density, $\boldsymbol{U}$ the velocity and ε the specific internal energy related to total energy E as $E = \varepsilon + \frac{U^2}{2}$. The previous system is equipped with a thermodynamics closure (equation of state EOS) providing the pressure $P = P(\rho, \varepsilon)$. The first two equations express the volume and momentum conservation equations.
Volume conservation equation is often referred to as the Geometrical Conservation Law (GCL). The last equations are the trajectory equations

$$\frac{d\boldsymbol{X}}{dt} = \boldsymbol{U}(\boldsymbol{X}(t), t), \quad \boldsymbol{X}(0) = \boldsymbol{x}, \tag{2}$$

expressing the Lagrangian motion of any point initially located at position $\boldsymbol{x}$.

2.2. Notation.

We use a staggered discretization (see figure 1). Position and velocity are defined at grid points while thermodynamical variables are located at cell centers. An unstructured grid consisting of a collection of non-overlapping polygons is considered. Each polygonal cell is assigned a unique index c and denoted Ω_c. Each vertex/point of the mesh is assigned a unique index p and we denote $C(p)$ the set of cells sharing a particular vertex p. A polygonal cell is subdivided into a set of subcells; each being uniquely defined by a pair of indices c and p and denoted Ω_{cp}. This subcell is constructed by connecting the cell center of Ω_c to the mid-points of cell edges impinging on point p. The union of subcells Ω_{cp} that share a particular vertex p allows to define the dual cell Ω_p related to point p with $\Omega_p = \bigcup_{c \in C(p)} \Omega_{cp}$. Previous notation defines the primary grid $\bigcup_c \Omega_c$ and the dual grid $\bigcup_p \Omega_p$. Primary cells Ω_c and dual cells Ω_p volumes are functions of time t. We make the fundamental assumption that the subcells are Lagrangian volumes. Namely the subcell mass m_{cp} is constant in time; knowing initial density field $\rho^0(\boldsymbol{X})$ one introduces the initial mean density in cell c as $\rho_c^0 = \int_{\Omega_c(0)} \rho^0(\boldsymbol{X}) d\boldsymbol{X} / V_c^0$, where V_c^0 is the volume of cell Ω_c at time $t = 0$. Subcell mass is defined as $m_{cp} = \rho_c^0 V_{cp}^0$ where V_{cp}^0 is the initial volume of subcell Ω_{cp}. By summation of Lagrangian subcell masses one defines Lagrangian cell/point masses as

$$m_c = \sum_{p \in \mathcal{P}(c)} m_{cp}, \quad \text{and} \quad m_p = \sum_{c \in C(p)} m_{cp}, \tag{3}$$

where $\mathcal{P}(c)$ is the set of counterclockwise ordered vertices of cell c.

2.3. Compatible discretization.

Following [6, 2] the momentum equation is semi-discretized in space over the dual cell Ω_p

$$m_p \frac{d}{dt}\boldsymbol{U}_p + \sum_{c \in C(p)} \boldsymbol{F}_{cp} = \boldsymbol{0}, \tag{4}$$

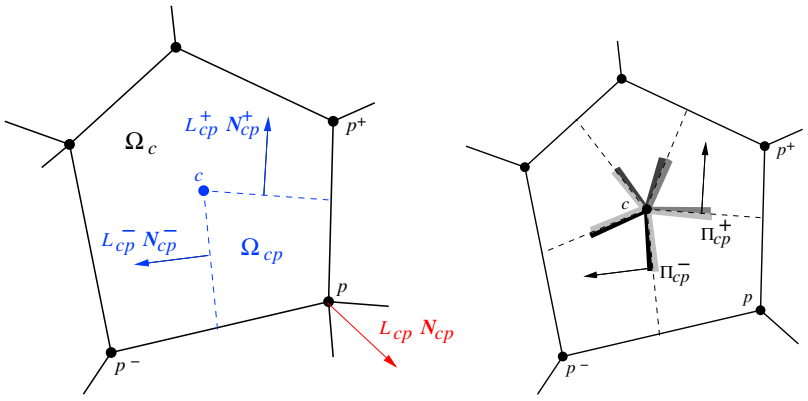

Figure 1: Left: Polygonal cell Ω_c subdivided into subcells Ω_{cp}. Points (subscript p) are counterclockwise ordered p^-, p, p^+. Outward unit normals of internal subcell boundaries: $\boldsymbol{N}^-_{cp}, \boldsymbol{N}^+_{cp}$. Internal edge lengths: L^-_{cp}, L^+_{cp}. Corner vector: $L_{cp}\boldsymbol{N}_{cp} = -L^-_{cp}\boldsymbol{N}^-_{cp} - L^+_{cp}\boldsymbol{N}^+_{cp}$. Right: Notation used in the cell-centered Riemann solver. Two pressures per subcell are introduced at the cell center: Π^+_{cp}, Π^-_{cp}. They are related to geometrical vectors $L^+_{cp}\boldsymbol{N}^+_{cp}$, $L^-_{cp}\boldsymbol{N}^-_{cp}$. Then $2 \times \mathcal{P}(c)$ pressures are introduced within cell Ω_c.

where $\boldsymbol{F}_{cp}$ is a fundamental object called *subcell force* from cell c that acts on point p and is defined as $\boldsymbol{F}_{cp} = \int_{\partial\Omega_p(t)\cap\Omega_c(t)} \boldsymbol{P}\boldsymbol{N}\mathrm{d}l$, so that $\sum_{c\in\mathcal{C}(p)} \boldsymbol{F}_{cp} = \int_{\partial\Omega_p} \boldsymbol{P}\boldsymbol{N}\mathrm{d}l$. Total momentum conservation (away from boundaries) is given in its discrete form by $\sum_p m_p \dfrac{d}{dt}\boldsymbol{U}_p = \boldsymbol{0}$, however (4) yields

$$\sum_p m_p \frac{d}{dt}\boldsymbol{U}_p = \sum_p \left(- \sum_{c\in\mathcal{C}(p)} \boldsymbol{F}_{cp} \right) = \boldsymbol{0}. \tag{5}$$

By switching the sums one finally exhibits the condition $-\sum_c \sum_{p\in\mathcal{P}(c)} \boldsymbol{F}_{cp} = \boldsymbol{0}$, and a sufficient cell-based condition is that the subcell forces acting in cell c sum up to zero: $\sum_{p\in\mathcal{P}(c)} \boldsymbol{F}_{cp} = \boldsymbol{0}$.
A semi-discrete internal energy equation that ensures total energy conservation is then derived. Away from boundary conditions, we introduce total kinetic energy at time $t > 0$ as a sum over the dual cells $\mathcal{K}(t) = \sum_p \frac{1}{2} m_p \boldsymbol{U}_p^2(t)$, and internal energy as $\mathcal{E}(t) = \sum_c m_c \varepsilon_c(t)$. Total energy is then defined as $E(t) = \mathcal{K}(t) + \mathcal{E}(t)$. The conservation of total energy (away from boundary conditions) writes

$$\frac{d}{dt}\mathcal{K} + \frac{d}{dt}\mathcal{E} = 0. \tag{6}$$

The substitution of kinetic and internal energies into (6) recalling that cell/point masses are Lagrangian objects, *i.e* they not depend on time, produces

$$\frac{d}{dt}\mathcal{K} + \frac{d}{dt}\mathcal{E} = \sum_c m_c \frac{d}{dt}\varepsilon_c + \sum_p m_p \frac{d}{dt}\boldsymbol{U}_p \cdot \boldsymbol{U}_p, \tag{7}$$

which, by substituting the semi-discrete momentum equation (4) yields

$$\sum_c m_c \frac{d}{dt}\varepsilon_c - \sum_p \sum_{c\in\mathcal{C}(p)} \boldsymbol{F}_{cp} \cdot \boldsymbol{U}_p = \sum_c \left(m_c \frac{d}{dt}\varepsilon_c - \sum_{p\in\mathcal{P}(c)} \boldsymbol{F}_{cp} \cdot \boldsymbol{U}_p \right) = 0, \tag{8}$$

the middle part of the previous equation is obtained by shifting sums into the work term. A sufficient condition for total energy conservation is obtained by requiring the previous equation to hold in each cell c, that is to say:

$$m_c \frac{d}{dt}\varepsilon_c - \sum_{p\in\mathcal{P}(c)} \boldsymbol{F}_{cp} \cdot \boldsymbol{U}_p = 0. \tag{9}$$

Once the subcell force is known then momentum and internal energy can be updated using equations (4) and (9). Total energy, momentum (and trivially mass) are conserved by construction *independently of the subcell force form*[2], and that masses are computed as (3). New position of point is updated *via* the trajectory equation. Since velocity is defined at point p, the GCL is satisfied and the volume equation writes

$$\frac{d}{dt}V_c \; + \sum_{p\in\mathcal{P}(c)} \left(L_{cp}^{-}\boldsymbol{N}_{cp}^{-} + L_{cp}^{+}\boldsymbol{N}_{cp}^{+}\right)\cdot\boldsymbol{U}_p = 0, \tag{10}$$

where V_c is the volume of cell c, The previous discretization is obtained by time differentiation of V_c, leading to a compatible discrete divergence operator over cell c as

$$(\nabla\cdot\boldsymbol{U})_c = \frac{1}{V_c}\sum_{p\in\mathcal{P}(c)} L_{cp}\boldsymbol{N}_{cp}\cdot\boldsymbol{U}_p, \tag{11}$$

where the unit corner vector is defined by $L_{cp}\boldsymbol{N}_{cp} = -L_{cp}^{-}\boldsymbol{N}_{cp}^{-} - L_{cp}^{+}\boldsymbol{N}_{cp}^{+}$ (see figure 1). Equation (10) is compatible with the discrete version of the trajectory equation (2): $\frac{d}{dt}\boldsymbol{X}_p = \boldsymbol{U}_p$.

2.4. Subcell force definition via entropy consideration

The only remaining unknown is the subcell force $\mathbf{F}_{cp}$. By manipulating the entropy equation we derive a general form of the subcell force in this section. Using Gibbs formula, the time rate of change of entropy in cell c writes

$$m_c T_c \frac{d}{dt}S_c = m_c\left[\frac{d}{dt}\varepsilon_c + P_c\frac{d}{dt}\left(\frac{1}{\rho_c}\right)\right]. \tag{12}$$

Substituting the time rate of change of internal energy (9) and volume leads to

$$m_c T_c \frac{d}{dt}S_c = \sum_{p\in\mathcal{P}(c)}\left(\boldsymbol{F}_{cp} + P_c L_{cp}\boldsymbol{N}_{cp}\right)\cdot\boldsymbol{U}_p. \tag{13}$$

For smooth flow entropy must be conserved, leading to the following subcell force decomposition

$$\boldsymbol{F}_{cp} = -P_c L_{cp}\boldsymbol{N}_{cp} + \boldsymbol{F}_{cp}^{\text{viscous}}. \tag{14}$$

The subtitution into (9) yields

$$m_c\left[\frac{d}{dt}\varepsilon_c + P_c\frac{d}{dt}\left(\frac{1}{\rho_c}\right)\right] = \sum_{p\in\mathcal{C}(p)}\boldsymbol{F}_{cp}^{\text{viscous}}\cdot\boldsymbol{U}_p. \tag{15}$$

and the second law of thermodynamics requires $\sum_{p\in\mathcal{P}(c)}\boldsymbol{F}_{cp}^{\text{viscous}}\cdot\boldsymbol{U}_p \geq 0$. Moreover viscous forces must vanish for smooth flows (e.g. rarefaction, isentropic compression). As previously shown momentum conservation requires the condition $\sum_{p\in\mathcal{P}(c)}\boldsymbol{F}_{cp} = \mathbf{0}$ which rewrites using (14)

$$\sum_{p\in\mathcal{P}(c)}\boldsymbol{F}_{cp} = \sum_{p\in\mathcal{P}(c)} -P_c L_{cp}\boldsymbol{N}_{cp} + \boldsymbol{F}_{cp}^{\text{viscous}} = -P_c\sum_{p\in\mathcal{P}(c)} L_{cp}\boldsymbol{N}_{cp} + \sum_{p\in\mathcal{P}(c)}\boldsymbol{F}_{cp}^{\text{viscous}} = \mathbf{0}.$$

Recalling that on a closed contour the geometrical relation $\sum_{p\in\mathcal{P}(c)} L_{cp}\boldsymbol{N}_{cp} = \mathbf{0}$ holds, we finally get the condition on subcell viscous forces

$$\sum_{p\in\mathcal{P}(c)}\boldsymbol{F}_{cp}^{\text{viscous}} = \mathbf{0}. \tag{16}$$

Let's remark that the Galilean invariance is ensured by this property as equation (15) is equivalent to $m_c\left[\frac{d}{dt}\varepsilon_c + P_c\frac{d}{dt}\left(\frac{1}{\rho_c}\right)\right] = \sum_{p\in\mathcal{C}(p)}\boldsymbol{F}_{cp}^{\text{viscous}}\cdot\left(\boldsymbol{U}_p - \boldsymbol{U}_c\right)$, where $\boldsymbol{U}_c$ is any constant velocity in cell c.

[2] providing that the sum of subcell forces in a cell is zero.

2.5. Artificial viscosity and Riemann solver

In classical staggered Lagrangian scheme artificial viscosity is a key point to handle shock wave and steep front. A lot of effort has been deployed since the 50's and the seminal work of von Neumann [9] to derive a proper artificial viscosity formulation. The viscosity is thought of as an extra pressure term denoted q. New developments in the 80's in [10] and late 90's in [4, 3] have been made but they consider the same basic roots.
In this work we consider artificial viscosity as produced thanks to a cell-centered approximation of a multidimensional Riemann problem. We introduce two pressures per subcell that are located at the cell center, they are called Π^-_{cp}, Π^+_{cp}. They are related to the unit outward normals $\boldsymbol{N}^+_{cp}$ and $\boldsymbol{N}^-_{cp}$ respectively (see figure 1). The subcell force written as a contour volume reads

$$\boldsymbol{F}_{cp} = \Pi^+_{cp} L^+_{cp} \boldsymbol{N}^+_{cp} + \Pi^-_{cp} L^-_{cp} \boldsymbol{N}^-_{cp}. \tag{17}$$

Pressures are obtained by solving half-Riemann problems in the normal directions

$$P_c - \Pi^+_{cp} = Z^+_{cp} \left(\boldsymbol{U}_c - \boldsymbol{U}_p \right) \cdot \boldsymbol{N}^+_{cp}, \qquad P_c - \Pi^-_{cp} = Z^-_{cp} \left(\boldsymbol{U}_c - \boldsymbol{U}_p \right) \cdot \boldsymbol{N}^-_{cp}, \tag{18}$$

where Z^+_{cp}, Z^-_{cp} are swept mass fluxes (namely the mass seen by a wave travelling with an approximation of the local shock speed), and $\boldsymbol{U}_c$ is the cell-centered velocity which remains to be defined. Using (18) the subcell force is recast into the form

$$\boldsymbol{F}_{cp} = \left(L^+_{cp} \boldsymbol{N}^+_{cp} + L^-_{cp} \boldsymbol{N}^-_{cp} \right) P_c - \mathsf{M}_{cp} \left(\boldsymbol{U}_c - \boldsymbol{U}_p \right), \tag{19}$$

where $\mathsf{M}_{cp} = Z^+_{cp} L^+_{cp} (\boldsymbol{N}^+_{cp} \otimes \boldsymbol{N}^+_{cp}) + Z^-_{cp} L^-_{cp} (\boldsymbol{N}^-_{cp} \otimes \boldsymbol{N}^-_{cp})$, is a 2×2 symmetric positive definite matrix. Consequently the viscous part of the force simply writes

$$\boldsymbol{F}^{\text{viscous}}_{cp} = -\mathsf{M}_{cp} \left(\boldsymbol{U}_c - \boldsymbol{U}_p \right). \tag{20}$$

The cell center velocity is determined by using the previously derived condition (16) together with the definition of viscous force (20) leading to

$$\sum_{p \in \mathcal{P}(c)} -\mathsf{M}_{cp} \left(\boldsymbol{U}_c - \boldsymbol{U}_p \right) = \boldsymbol{0} \quad \Longleftrightarrow \quad \mathsf{M}_c \boldsymbol{U}_c = \sum_{p \in \mathcal{P}(c)} \mathsf{M}_{cp} \boldsymbol{U}_p, \tag{21}$$

where $\mathsf{M}_c = \sum_{p \in \mathcal{P}(c)} \mathsf{M}_{cp}$. Equation (21) is a 2×2 non-linear system which can be solved utilizing an iterative algorithm. The non-linearity comes from the swept mass fluxes, that, following Dukowicz [7, 8], one approximates as

$$Z^+_{cp} = \rho_c \left[\sigma_c + c_Q \Gamma_c \mid (\boldsymbol{U}_c - \boldsymbol{U}_p) \cdot \boldsymbol{N}^+_{cp} \mid \right], \quad Z^-_{cp} = \rho_c \left[\sigma_c + c_Q \Gamma_c \mid (\boldsymbol{U}_c - \boldsymbol{U}_p) \cdot \boldsymbol{N}^-_{cp} \mid \right]. \tag{22}$$

Here, σ_c is the isentropic sound speed, c_Q a user-defined parameter (set to 1 in our simulations) and Γ_c a material dependent coefficient, which for a γ gas law can be defined by

$$\Gamma_c = \begin{cases} \frac{\gamma+1}{2} & \text{if} \quad (\nabla \cdot \boldsymbol{U})_{cp} < 0, \\ 0 & \text{if} \quad (\nabla \cdot \boldsymbol{U})_{cp} \geq 0, \end{cases} \tag{23}$$

where $(\nabla \cdot \boldsymbol{U})_{cp} = -\frac{1}{V_{cp}} L_{cp} \boldsymbol{N}_{cp} \cdot (\boldsymbol{U}_c - \boldsymbol{U}_p)$ is the subcell contribution to the velocity divergence. In case of rarefaction we recover the acoustic approximation whereas in case of shock wave we get a two-shock approximation. Once $\boldsymbol{U}_c$ is known we can compute the subcell force with (19). The entropy inequality is fulfilled as matrices M_{cp} are positive definite and the substitution of the viscous part of the subcell force $\boldsymbol{F}^{\text{viscous}}_{cp}$ into (15) yields

$$m_c \left[\frac{d}{dt} \varepsilon_c + P_c \frac{d}{dt} \left(\frac{1}{\rho_c} \right) \right] = \sum_{p \in \mathcal{C}(p)} -\mathsf{M}_{cp} \left(\boldsymbol{U}_c - \boldsymbol{U}_p \right) \cdot \left(\boldsymbol{U}_c - \boldsymbol{U}_p \right) \;\geq\; 0. \tag{24}$$

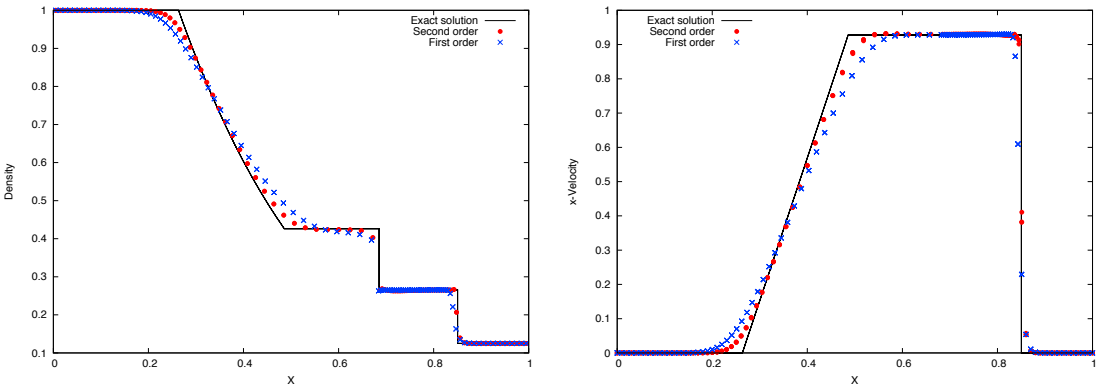

Figure 2: 1D Sod shock tube problem at $t = 0.2$ with 100 cells. From left to right: Cell density, x-component of nodal velocity. First order proposed scheme $\times$ and second order scheme $\bullet$ *vs* the exact solution (line).

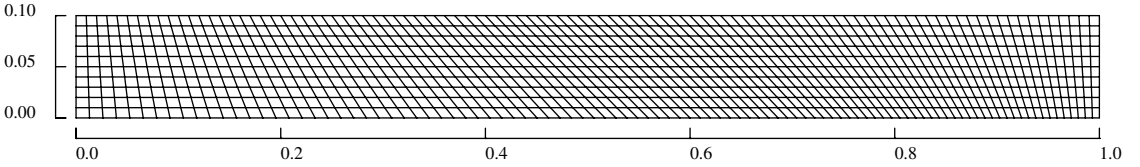

Figure 3: Initial skewed mesh used for the Saltzman problem made of 100×10 cells.

3. Second order extension

Second order extension in space is obtained using an extrapolated velocity inside the subcell force computation. First a piecewise linear reconstruction of the velocity field on the dual cells is built:

$$\widetilde{\boldsymbol{U}}_p(\boldsymbol{X}) = \boldsymbol{U}_p + \nabla \boldsymbol{U}_p \cdot \left(\boldsymbol{X} - \boldsymbol{X}_p\right). \tag{25}$$

The construction on the dual grid allows to define $|\mathcal{P}(c)|$ extrapolated velocities at cell-center $\boldsymbol{X}_c$ that are later used in the Riemann solver. The slopes $\nabla \boldsymbol{U}_p$ are solutions of the least squares problem

$$\nabla \boldsymbol{U}_p = \arg\min \sum_{p' \in \mathcal{N}(p)} \left(\left(\boldsymbol{U}_{p'} - \boldsymbol{U}_p\right) - \nabla \boldsymbol{U}_p \left(\boldsymbol{X}_{p'} - \boldsymbol{X}_p\right) \right)^2, \tag{26}$$

where $\mathcal{N}(p)$ is the set of neighbor vertices of vertex p. The previous least squares problem can indeed be recast into a linear system form as

$$\nabla \boldsymbol{U}_p = \mathsf{M}_p^{-1} \left(\sum_{p' \in \mathcal{N}(p)} (\boldsymbol{U}_{p'} - \boldsymbol{U}_p) \otimes (\boldsymbol{X}_{p'} - \boldsymbol{X}_p) \right), \tag{27}$$

where matrix M_p is the symmetric positive definite matrix $\mathsf{M}_p = \sum_{p' \in \mathcal{N}(p)} (\boldsymbol{X}_{p'} - \boldsymbol{X}_p) \otimes (\boldsymbol{X}_{p'} - \boldsymbol{X}_p)$. Monotonicity is achieved thanks to the classical Barth Jespersen slope limiter [1]. Then the Riemann problem in its second-order version is solved using the velocity extrapolated from the vertices to the cell center. That is to say equation (21) becomes

$$\boldsymbol{U}_c = \mathsf{M}_c^{-1} \sum_{p \in \mathcal{P}(c)} \mathsf{M}_{cp} \widetilde{\boldsymbol{U}}_p(\boldsymbol{X}_c). \tag{28}$$

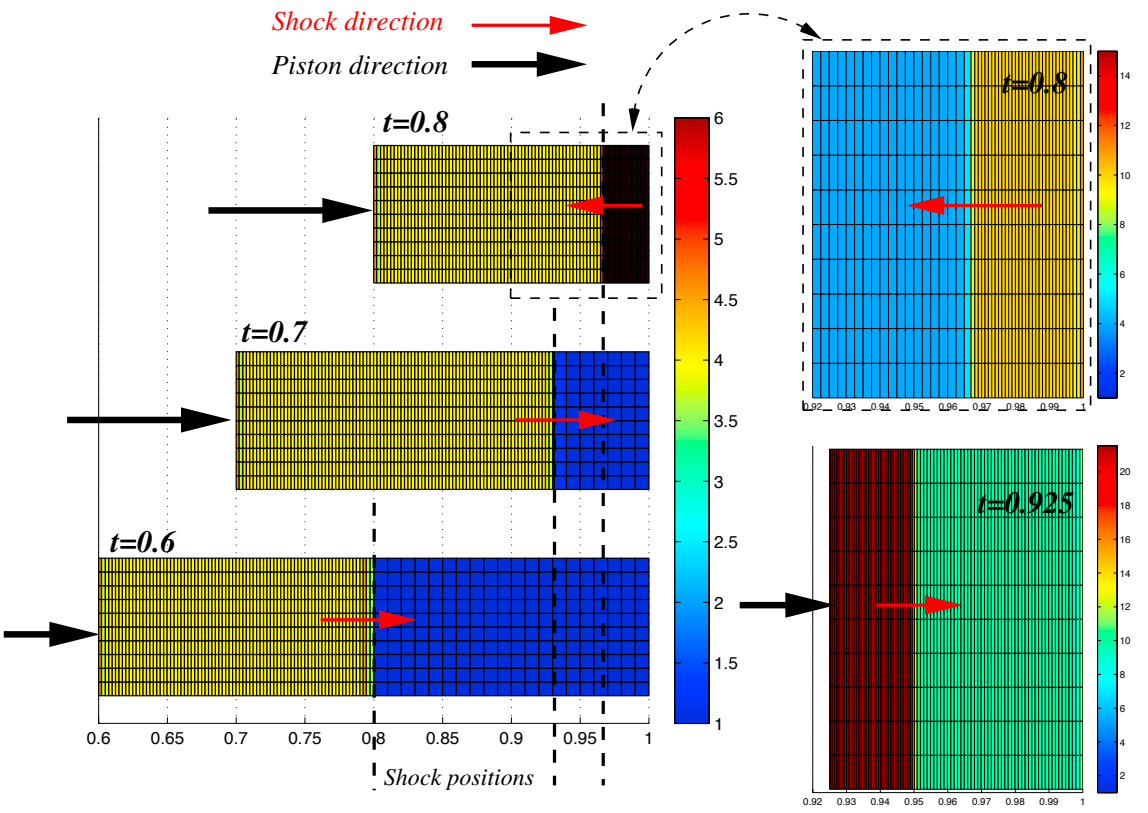

Figure 4: Piston problem — Left hand side: Density map and mesh $t = 0.6$: Exact shock location is $x = 4/5$, post-shock density is $\rho = 4$. $t = 0.7$: Exact shock location is $x = 14/15$, post-shock density is $\rho = 4$ $t = 0.8$: Exact shock location is $x = 29/30$, post-shock density is $\rho = 10$. Right hand side: zoom at $t = 0.8$ (top) and final time $t = 0.925$ (bottom, post-shock density is $\rho = 20$).

Subcell forces (20) are modified accordingly. $\boldsymbol{F}_{cp} = \left(L^+_{cp}\boldsymbol{N}^+_{cp} + L^-_{cp}\boldsymbol{N}^-_{cp}\right) P_c - \mathsf{M}_{cp}\left(\boldsymbol{U}_c - \widetilde{\boldsymbol{U}}_p(\boldsymbol{X}_c)\right)$. The time discretization is performed with a classical two-step predictor-corrector scheme. The full discretization in space and time is presented hereafter.

Predictor step.

1. Compute $\boldsymbol{U}^n_c$ with the cell-centered Riemann solver: $\boldsymbol{U}^n_c = (\mathsf{M}^n_c)^{-1} \sum_{p\in\mathcal{P}(c)} \left(\mathsf{M}^n_{cp}\widetilde{\boldsymbol{U}}^n_p(\boldsymbol{X}^n_c)\right)$,
2. Compute subcell forces: $\boldsymbol{F}^n_{cp} = \left(L^+_{cp}\boldsymbol{N}^+_{cp} + L^-_{cp}\boldsymbol{N}^-_{cp}\right)^n P^n_c - \mathsf{M}^n_{cp}\left(\boldsymbol{U}^n_c - \widetilde{\boldsymbol{U}}^n_p(\boldsymbol{X}^n_c)\right)$.
3. Update internal energy: $m_c\left(\varepsilon^{n+1/2}_c - \varepsilon^n_c\right) - \frac{\Delta t}{2}\sum_{p\in\mathcal{P}(c)} \boldsymbol{F}^n_{cp}\cdot\boldsymbol{U}^n_p = 0$.
4. Update vertex position: $\boldsymbol{X}^{n+1/2}_p = \boldsymbol{X}^n_p + \frac{\Delta t}{2}\boldsymbol{U}^n_p$.
5. Update volume and density: $\rho^{n+1/2}_c = \frac{m_c}{V^{n+1/2}_c}$, $\quad \rho^{n+1/2}_{cp} = \frac{m_{cp}}{V^{n+1/2}_{cp}}$.
6. Compute predicted pressures: $P^{n+1/2}_c = P(\rho^{n+1/2}_c, \varepsilon^{n+1/2}_c)$.

Corrector step.

1. Compute $\boldsymbol{U}^{n+1/2}_c$ with the Riemann solver: $\boldsymbol{U}^{n+1/2}_c = \left(\mathsf{M}^{n+1/2}_c\right)^{-1} \sum_{p\in\mathcal{P}(c)} \left(\mathsf{M}^{n+1/2}_{cp}\widetilde{\boldsymbol{U}}^{n+1/2}_p(\boldsymbol{X}^{n+1/2}_p)\right)$,
2. Compute subcell forces: $\boldsymbol{F}^{n+1/2}_{cp} = \left(L^+_{cp}\boldsymbol{N}^+_{cp} + L^-_{cp}\boldsymbol{N}^-_{cp}\right)^{n+1/2} P^{n+1/2}_c - \mathsf{M}^{n+1/2}_{cp}\left(\boldsymbol{U}^{n+1/2}_c - \widetilde{\boldsymbol{U}}^{n+1/2}_p(\boldsymbol{X}^{n+1/2}_c)\right)$.

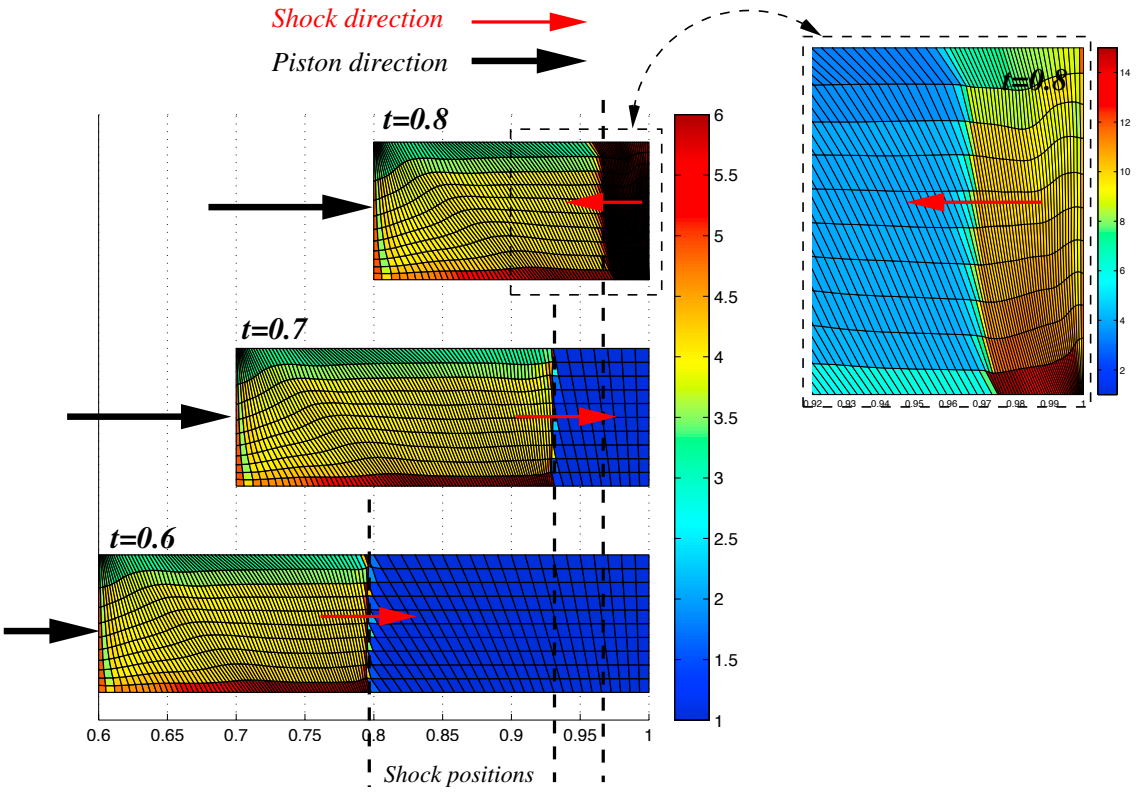

Figure 5: Saltzman problem — Left hand side: Density map and mesh $t = 0.6$: Exact shock location is $x = 4/5$, post-shock density is $\rho = 4$. $t = 0.7$: Exact shock location is $x = 14/15$, post-shock density is $\rho = 4$ $t = 0.8$: Exact shock location is $x = 29/30$, post-shock density is $\rho = 10$, the maximum numerical cell density is around 20. Right hand side: zoom at $t = 0.8$.

3. Update momentum: $m_p \left(\boldsymbol{U}_p^{n+1} - \boldsymbol{U}_p^n\right) + \Delta t \ \sum_{c \in \mathcal{C}(p)} \boldsymbol{F}_{cp}^{n+1/2} = \boldsymbol{0}$.
4. Update internal energy: $m_c \left(\varepsilon_c^{n+1} - \varepsilon_c^n\right) - \Delta t \ \sum_{p \in \mathcal{P}(c)} \boldsymbol{F}_{cp}^{n+1/2} \cdot \boldsymbol{U}_p^{n+1/2} = 0$, with $\boldsymbol{U}_p^{n+1/2} = \frac{1}{2}(\boldsymbol{U}_p^{n+1} + \boldsymbol{U}_p^n)$.
5. Update vertex position: $\boldsymbol{X}_p^{n+1} = \boldsymbol{X}_p^n + \Delta t \ \boldsymbol{U}_p^{n+1/2}$.
6. Update volume and density: $\rho_c^{n+1} = \frac{m_c}{V_c^{n+1}}, \quad \rho_{cp}^{n+1} = \frac{m_{cp}}{V_{cp}^{n+1}}$.
7. Compute pressures: $P_c^{n+1} = P(\rho_c^{n+1}, \varepsilon_c^{n+1})$,

4. Numerical results

The first test problem is the classical 1D Sod shock tube. On domain $[0, 1]$ are initialized a left $(\rho_L, u_L, p_L) = (1, 0, 1)$ and right state $(\rho_R, u_R, p_R) = (0.125, 0, 0.1)$ of a perfect gas with $\gamma = 7/5$ separated at $\boldsymbol{X} = 0.5$. Symmetry boundary conditions are considered and the final time is $t = 0.2$. Figure 2 shows the cell-centered density, and nodal x-component of nodal velocity for the first order scheme $\times$ and the second order scheme $\bullet$ *vs* the exact solution (line). The improvement gained by the second order extension in space and time is clear.

The second test is the 2D Saltzman problem. The computational domain is $[0, 1] \times [0, 0.1]$. Initial conditions are $(\rho^0, P^0, \boldsymbol{U^0}) = (1, 10^{-6}, 0)$ for a gamma law gas with $\gamma = 5/3$. A piston which velocity is $U^\star = 1$ is imposed as a boundary condition at $x = 0$ (symmetry boundary conditions otherwise). This problem is by nature 1D and an exact solution exists up to $t < 1$. As a sanity check we verified that on a 100×10 perfect quadrangular mesh aligned with

the shock direction the proposed scheme perfectly reproduces the 1D symetry, see Figure 4 up to final time $t = 0.925$. The Saltzman problem considers a 100×10 square mesh that is skewed as presented in Figure 3 (see [8] for the details to build this mesh). Such a mesh has a tendency to produce numerical vorticity and/or oscillations that may become lethal to Lagrangian schemes. Consequently this problem is a robustness test. Times $t = 0.6, 0.7$ and $t = 0.8$ are considered. Results are presented in Figure 5. The results on this robustness test are not totally satisfactory as the mesh tangles soon after $t = 0.8$. One expects to improve this result by adding some stabilization procedure through the use of subpressure as in [5]. However up to this time the exact shock position and exact density plateaus are quite well reproduced.

5. Conclusion

In this work we developed a new family of staggered Lagrangian schemes devoted to solve compressible hydrodynamics equations. This family has been recast into the classical compatible formulation [6, 2]. By using the concept of approximate cell-centered Riemann problem (see [8] and references herein) one develops a new derivation for the artificial viscosity. Artificial viscosity concept was previously based on *ad hoc* techniques [9, 10, 4, 3]. In our new formulation the cornerstone is a subcell-based positive definite matrix that is acting on the velocity difference between the subcell associated cell center and node. One example of such a matrix is proposed in this paper. We extended the family to second order in space by using piecewise linear reconstruction of velocity field, and, second order in time by a predictor-corrector scheme. We showed that effective second order is gained on the Sod problem and presented only the demanding example of Saltzman piston. In the future we will analytically and numerically study different choices of matrix and their link to existing work. Finally the axi-symmetric, 3D and Arbitrary-Lagrangian-Eulerian extensions of this family are planed to be investigated.

References

[1] T.J. Barth, D.C. Jespersen, The design and application of upwind schemes on unstructured meshes, AIAA Paper **89-0366**, 1–12, (1989)
[2] A.L. Bauer, D.E. Burton, E.J. Caramana, R. Loubère, M.J. Shashkov, P.P. Whalen,, The internal consistency, stability, and accuracy of the discrete, compatible formulation of Lagrangian hydrodynamics, J. Comput. Phys. **218** (2006) 572.
[3] J.C. Campbell, M.J. Shashov, A tensor artificial viscosity using a mimetic finite difference algorithm, J. Comput. Phys. **172** (2001) 739.
[4] E.J. Caramana, M.J. Shashkov, P.P. Whalen, Formulations of Artificial Viscosity for Multidimensional Shock Wave Computations, J. Comput. Phys. **144** (1998) 70.
[5] E.J. Caramana, M.J. Shashkov, Elimination of artificial grid distorsion and hourglass–type motions by means of Lagrangian subzonal masses and pressures, J. Comput. Phys. **142** (1998) 521.
[6] E.J. Caramana, D.E. Burton, M.J. Shashkov, P. P. Whalen, The construction of compatible hydrodynamics algorithms utilizing conservation of total energy, J. Comput. Phys. **146** (1998) 227.
[7] J.K. Dukowicz, A general, non-iterative Riemann solver for Godunov's method, J. Comput. Phys. **61** (1985) 119.
[8] P.-H. Maire, A high-order cell-centered Lagrangian scheme for two-dimensional compressible fluid flows on unstructured mesh, J. Comput. Phys. **228** (2009) 2391
[9] J. Von Neumann, R.D. Rychtmyer, A method for the numerical calculation of hydrodynamic shocks, J. Appl. Phys. 21 (1950) 232.
[10] M.L. Wilkins, Use of Artificial Viscosity in Multidimensional Fluid Dynamic Calculations, J. Comput. Phys. **36** (1980) 281.